# Comparative Study of Influence of Experimental Configuration on Densities of Active Species in the Early Afterglows of N2/(0–2.5%)H2 HF Flowing Plasmas

M Abdeladim, Jean-Philippe Sarrette, J Amorim, André Ricard

Plasma Chemistry and Plasma Processing (2022) 42:1201–1210
https://doi.org/10.1007/s11090-022-10272-0

ORIGINAL PAPER

# Comparative Study of Influence of Experimental Configuration on Densities of Active Species in the Early Afterglows of $N_2$/(0–2.5%)$H_2$ HF Flowing Plasmas

**M. Abdeladim[1] · J. P. Sarrette[2] · J. Amorim[3] · A. Ricard[2]**

Received: 21 February 2022 / Accepted: 10 June 2022 / Published online: 16 July 2022


**Abstract**
Afterglows of mixed gas of $N_2$ and $H_2$(0–2.5%) flowing microwave discharges in a 5 mm diameter tube connected to a 5 L reactor via a tube of 1.8 cm diameter and 50 cm long, have been studied using optical emission spectroscopy. The obtained results at the entrance of the afterglow tube of 1.8 cm diameter: Short time afterglow (SA), ($10^{-3}$ s) and inside the 5 L reactor: Long time afterglow (LA), ($10^{-2}$ s) were then compared. It was found that, in $N_2$ at 2 Torr, 0.5 slpm, the active specie density ratios had a constant value of $10^{-2}$ for $N/N_2$, but decreased respectively from $10^{-3}$ to $10^{-4}$ for $N_2$ (X,v > 13)/$N_2$ and from $10^{-6}$ to $10^{-8}$ for $N^+_2$ /$N_2$. By directly connecting the discharge tube inside the 5 L reactor, the density increases by 10 for $N_2$ (X,v > 13) and by $10^2$ for $N_2^+$ by changing the afterglow from LA($10^{-2}$ s) to a SA($10^{-3}$ s). Moreover and by adding 1% of $H_2$ to $N_2$, the $N/N_2$ and $H/H_2$ ratios had constant values of 1% and 0.2% respectively. The SA($10^{-3}$ s) appeared to be more efficient for surface treatments than the LA ($10^{-2}$ s).

**Keywords** $N_2$-$H_2$ microwave discharges · N-atoms · $N_2$ metastable molecules · $N_2^+$ ions · NH radicals and H-atoms

## Introduction

Afterglows of $N_2$ flowing microwave discharges have been previously studied at medium gas pressures (1–20 Torr) for sterilization of medical instruments by N-atoms [1, 2]. The effect of the introduction of a low percentage of $H_2$ into $N_2$ on the paper surface wettability was also previously investigated in the early afterglow [3]. A slight maximum of the N-atom density in the $N_2$/0.4%$H_2$ afterglow at 2 Torr, 1 slpm, 100 Watt was correlated to an increase of surface wettability.

✉ M. Abdeladim
mabdeladim@hotmail.com

[1] LMSE, Faculté de Génie Electrique, U.S.T.O, BP 1505, El Mnaour-Oran, Algeria

[2] UPS, INP; LAPLACE (Laboratoire Plasma et Conversion d'Energie), Université de Toulouse, 118 route de Narbonne, 31062 Toulouse, France

[3] Department Fisica, Instituto Tecnológico de Aeronautica, CTA, São José dos Campos 12228-900, Brazil

In the present study, the early afterglow flowing from $N_2$/(0–2.5%) $H_2$ microwave plasmas is studied with two different experimental configurations, the first set up is the same as the one already reported in [4]. The second set up is having a new experimental arrangement [5] in which a direct connection with the microwave flowing plasma to the reactor chamber is achieved. With this new set-up, the time necessary for the gas to flow between the discharge and the reactor (post-discharge time) was reduced from $2 \times 10^{-2}$ s to $(1–3) \times 10^{-3}$ s at 2 Torr, 0.5–1.0 slpm.

For this second configuration, it was expected to add to N-atoms other $N_2$ active species: $N_2(A)$, $N_2$ (X,v > 13) metastable molecules, $N_2^+$ ions, NH radicals and H-atoms in the post-discharge chamber. The importance of two configurations *i.e.* different afterglow residence times which play a crucial role in the generated species were made in evidence.

Intensities emitted by the $N_2$ 1st positive system at 580 nm ($N_2(B,11) \rightarrow N_2(A,7)$ vibrational band) and by the $N_2$ 2nd positive system at 316 nm ($N_2(C,1) \rightarrow N_2(B,0)$ vibrational band) are measured to obtain the N–atoms, $N_2(A)$, $N_2(X,v > 13)$ metastable molecules and $N_2^+$ ions absolute densities after NO titration to calibrate the N-atom densities [3]. From the NH($A \rightarrow X$) bands at 336 nm, the possibility to evaluate the NH radical and H-atom densities is analyzed by choosing the appropriated kinetic reactions at the origin of NH 336 nm emission.

## Experimental Setup

The first experimental setup is reported in previous works [1–3, 5]. It is reproduced in Fig. 1.

The discharge is located inside a 5 mm diameter tube and a length of 20 cm after the surfatron gap. The discharge tube is connected to a bent tube of 18 mm diameter and 50 cm length before a 5 L reactor where the previous surface treatments occurred [1–3]. The residence time of the afterglow in the 18 mm tube diameter before the 5 L reactor is in the range of $10^{-3}$–$10^{-2}$ s.

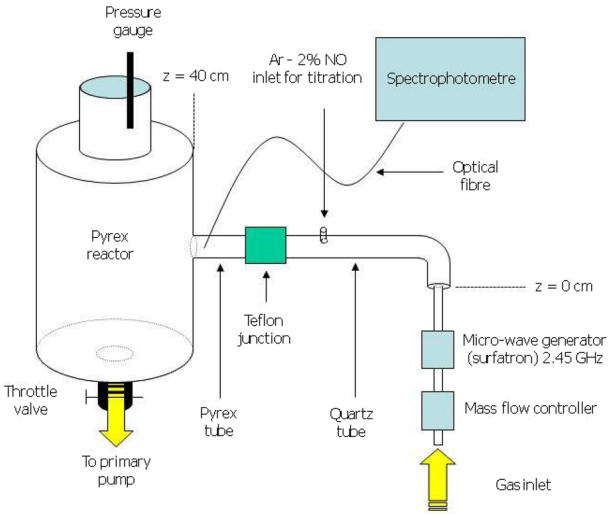


**Fig. 1** Microwave discharge in a tube of diameter 5 mm, length 20 cm and in a post-discharge bent tube of diameter 18 mm, length 30 cm connected to a 5 L reactor

A pink afterglow is observed in the bent part of the 18 mm tube with pure $N_2$ at 0.5 slpm, $p = 5$ Torr and 100 Watt. The NO titration of N-atoms in the late afterglows was performed by introducing an Ar-1.5%NO flow after the pink afterglow. At 8 Torr, 0.5 slpm and 100 Watt, $z = 3$ cm, a N-atom density of $1.0 \times 10^{15}$ $cm^{-3}$ was previously obtained [5].

The experimental setup of Fig. 1 has been modified as shown in Fig. 2 to directly introduce the 5 mm int. diameter discharge tube inside the 5 L reactor. The afterglow residence time at the entrance of the 5 L reactor was then reduced to $(1–3) \times 10^{-3}$ s [6, 7] as for the early afterglow at $z = 3$ cm in Fig. 1.

The aim of the present study is to compare the density of the $N_2$-$H_2$ active species, firstly in conditions of the same afterglow times ($10^{-3}$ s) and secondly with two afterglow times: $10^{-3}$ s and $10^{-2}$ s to check the capacity of the setup shown in Fig. 2 to treat surfaces in the reactor. The importance of the two configurations is to extend the afterglow residence time which plays a crucial role in the generated species, as seen in Table 2.

The $N_2$-$H_2$ microwave plasma is produced by a surfatron cavity at 2450 MHz, 100–200 Watt, 0.5–2 slpm at pressure from 2 to 8 Torr. At 2 Torr, a satisfactory diffusion of the afterglow is produced inside the whole 5 L reactor.

The optical emission spectroscopy across the reactor is performed by means of an optical fiber connected to an Acton Spectra Pro 2500i spectrometer (grating 600 g/mm) equipped with a Pixis 256E CCD detector (front illuminated $1024 \times 256$ pixels).

The N–atom density is obtained from the $I_{580}$ measured intensity after calibration by NO titration with a mixed gas of Ar and NO(1.5%) introduced across the 18 mm diameter tube as shown in Fig. 1.

## Kinetic Equations of Active Species in the Mixed Gas of $N_2$ and $H_2$(0–2.5%) Early Afterglow

### N-Atom Density

The pure late afterglow emission is produced by a dominant N + N recombination.

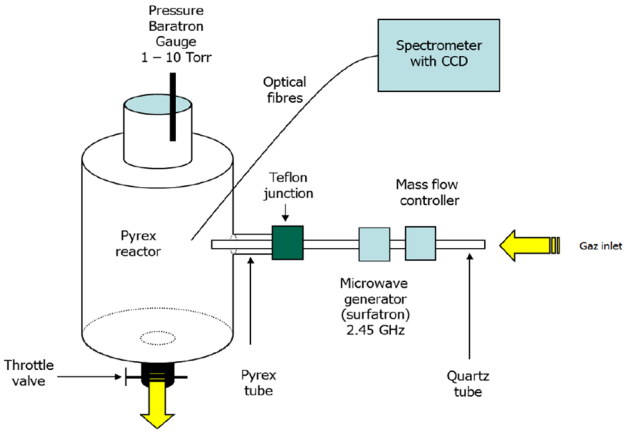


**Fig. 2** Microwave discharge in a tube of diameter 5 mm, length 20 cm directly connected to a 5 L reactor

The $N_2$ 580 nm band head intensity ($I_{580}$), in arbitrary unit, was measured for constant parameters of the Acton spectrometer (grating 600 gr/mm, entrance slit width of 150 µm and integrating time of 1 s).

$I_{580}$ is related to the N-atom density [N] as follows:

$$I_{580} = k_1 \cdot [\mathrm{N}]^2 \tag{1}$$

$$\text{with } k_1 = c(580) \cdot V \cdot (h \cdot c/580) \cdot A(580) \cdot k_a \cdot [\mathrm{M}] / \left( \upsilon^{\mathrm{R}}_{\mathrm{B},11} + [\mathrm{N}_2] \cdot k^{\mathrm{N2}}_{\mathrm{B},11} \right) \tag{2}$$

As mentioned in [6, 7], it is expressed in $k_1$:

The spectral response $c(580)$ of spectrometer (ratio of measured and true intensities at $\lambda = 580$ nm of tungsten lamp), $h$ and $c$ are respectively the constant of Planck and the light velocity, 580 is for $\lambda = 580$ nm, $V$ the afterglow volume observed by the optical fiber of the spectrometer, $A(580)$ the Einstein coefficient of the $N_2$ (580 nm) transition. The term $c(580) \cdot h \cdot c/580$ is in arbitrary unit.

$\upsilon^{\mathrm{R}}{}_{\mathrm{B},11}$ and $k^{\mathrm{N2}}{}_{\mathrm{B},11}$ are respectively the radiative frequency and the quenching rate constant of $N_2$ (B,11) by $N_2$.

The $k_a$ coefficient is for the following recombination reaction:

$$\mathrm{N} + \mathrm{N} + \mathrm{N}_2 \rightarrow \mathrm{N}_2(\mathrm{B}, \mathrm{v}' = 11) + \mathrm{N}_2 \tag{3}$$

In $k_1$, $c(580)$ is the spectral response of the used spectrometer, $A(580) = (7.8–9.6) \times 10^4\ \mathrm{s}^{-1}$ [8, 9], $k_a = 4.4 \times 10^{-33}\ \mathrm{cm}^6\mathrm{s}^{-1}$ [10], $\upsilon^{\mathrm{R}}{}_{\mathrm{B},11} = (2–2.4) \times 10^5\ \mathrm{s}^{-1}$ [8, 9] and $k^{\mathrm{N2}}{}_{\mathrm{B},11} = 3 \times 10^{-11}\ \mathrm{cm}^3\mathrm{s}^{-1}$ [11].

The fraction $a_{N+N}$ of the N + N recombination in the $I_{580}$ intensity has been determined in [6, 7] with the conditions of mixed pink and late afterglows ($a_{N+N} = 1$ in pure late afterglow with a dominant reaction (3) and $a_{N+N} = 0$ in pure pink afterglow with a minor reaction (3)). Therefore, Eq. (1) becomes:

$$a_{\mathrm{N+N}} \cdot \mathrm{I}_{580} = k_1 \cdot [\mathrm{N}]^2 \tag{4}$$

With $a_{N+N} \cdot I_{580}$ is the fraction $a_{N+N}$ of the measured intensity $I_{580}$ at emission of the early afterglow.

The N-atom absolute density was calibrated by NO titration and was determined from Eq. (4) by measuring $a_{N+N} \cdot I_{580}$ with constant spectrometer parameters.

The uncertainty on the N-atom density determination is estimated to be 30%.

By introducing directly the discharge tube of diameter 5 mm in the post-discharge reactor of 5 L (Fig. 2), an afterglow jet is produced along the whole reactor chamber at pressures of 6–8 Torr, flow rates 0.5–1.0 slpm and injected microwave power of 200 Watt.

The jet disappeared when the gas pressure was reduced to 2 Torr in $N_2/2.5\%H_2$ for the 0.5 slpm flow rate and power of 200 Watt. These plasma conditions were taken in the following for an afterglow diffusion in the whole 5 L chamber.

At 2 Torr, 0.5 slpm, $N_2/1\%H_2$, 200 Watt, it is found that $a_{N+N} = 0.85$ and $[\mathrm{N}] = 6 \times 10^{14}\ \mathrm{cm}^{-3}$ from Eq. (4). With $a_{N+N} = 0.85$, it can be considered that the afterglow was a nearly pure late afterglow (at 85%).

### Densities of $N_2(A)$, $N_2(X,v>13)$ and $N_2^+$

The line intensity ratio method [4, 12] is applied to determine the density of $N_2(A)$ ([A]) from that of N-atoms, by comparing the $I_{316}$ and $a_{N+N}{\cdot}I_{580}$ intensities,

where $I_{316}$ is the intensity emitted from the $N_2(C,v=1)$ radiative state. In the afterglow, the following dominant reaction is considered:

$$N_2(A) + N_2(A) \rightarrow N_2(C, v = 1) + N_2(X) \tag{5}$$

As reported in [13], the $a_{N+N}{\cdot}I_{580}$ / $I_{316}$ intensity ratio is as follows:

$$a_{N+N}{\cdot}I_{580}/I_{316} = k_3{\cdot}([N]/[A])^2 \tag{6}$$

*The value of* $k_3$ is $2.5 \times 10^{-7}$ taken from [13].

The density of all $N_2(X,v>13)$ molecules ([X, v > 13]) has been obtained by comparing the fractions of late and pink afterglows in the $I_{580}$ intensity: as reported in [13], $a_{N+N}{\cdot}I_{580}$ for the late (Eq. (4)) and $(1\text{-}a_{N+N}){\cdot}I_{580}$ for the pink where it is considered the following dominant reaction:

$$N_2(A) + N_2(X, v > 13) \rightarrow N_2(B, v = 11) + N_2(X) \tag{7}$$

It comes:

$$a_{N+N}/\left(1 - a_{N+N}\right) = k_4 \cdot [N]^2/[A] \cdot [X,\ v > 13] \tag{8}$$

*The value of* $k_4$ is $4\text{–}5 \times 10^{-6}$ determined from [11].

The $N_2^+$ ions density ($[N_2^+]$) is determined by comparing the $I_{316}$ intensity from reaction (5) with the $I_{391}$ intensity coming from the $N_2^+(B,v=0)$ radiative state excited by the following reaction [13]:

$$N_2^+(X) + N_2(X, v > 12) \rightarrow N_2^+(B, v = 0) + N_2(X) \tag{9}$$

The $I_{391}$ / $I_{316}$ intensity ratio is defined as follows:

$$I_{391}/I_{316} = k_5{\cdot}\left(\left[N_2^+\right][X,\ v > 13]\right)/[A]^2 \tag{10}$$

where it is taken the same value for the [X, v > 12] and [X, v > 13] densities.

*The value of* $k_5$ is $1.6{\times}10^{-2}$ defined in [11].

From the N-atom density of $6{\times}10^{14}$ $cm^{-3}$, at 2 Torr, 0.5 slpm, for an afterglow time of $(1\text{–}3){\times}10^{-3}$ s in the 5 L reactor, with $N_2$-1%$H_2$, 200 Watt, the following densities: $[A]=4{\times}10^{10}$ $cm^{-3}$, $[X, v>13]=1\ 10^{13}$ $cm^{-3}$ and $[N_2^+]=3{\times}10^9$ $cm^{-3}$ are obtained from Eqs. (6, 8 and 10).

### Densities of NH Radicals and H-atoms

The kinetics reactions at the origin of the NH(A) emission shown in Fig. 3 are analyzed.

It is first considered that the NH(A) radiative states in $N_2$–$H_2$ afterglows can be produced by the recombination of N and H atoms. However, the reaction coefficient producing the NH(A) state is unknown. Only the coefficient $k_e$ of the following full reaction:

$$N + H + M \rightarrow NH + M \tag{11}$$

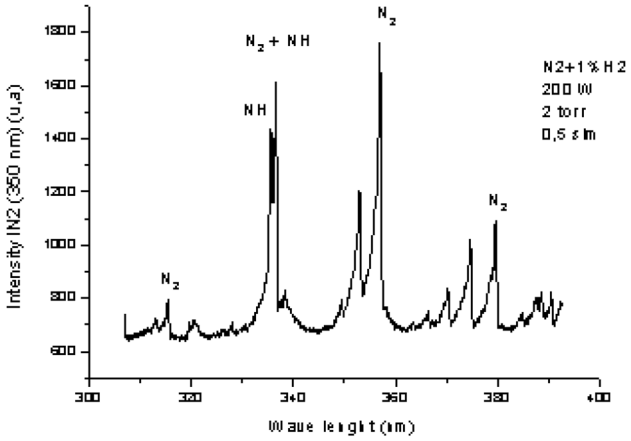


**Fig. 3** Spectrum of the $N_2$-1%$H_2$ afterglow in the 5 L reactor (Fig. 2) at $10^{-3}$ s, 2 Torr, 0.5 slpm and 200 Watt

where M = $N_2$ as reported in [14], with $k_e = 5(\pm 3)10^{-32}$ cm$^6$ s$^{-1}$.

By considering the NH potential curves [15], the NH(A,v = 0) vibrational level is almost at the same N + H dissociation energy (3.8–4.0 eV). Moreover, a NH($^5\Sigma^-$) repulsive curve is crossing NH($A^2\Pi$) at 4.2 eV. As a consequence, there is a potential barrier which inhibits the production of NH(A,v = 0) by the N + H recombination.

By comparing with the $N_2/O_2$ gas mixtures, the NO(B,0) level being 0.9 eV is lower than the N + O dissociation (6.5 eV), the reaction N + O + M → NO(B,0) + M is exothermic with a rate coefficient of $3 \times 10^{-34}$ cm$^6$ s$^{-1}$ [6, 7].

By taking into account now the $N_2$(X,v) + NH → $N_2$ + NH(A,v = 0) reaction, it is observed that the excitation of the NH(A,0) level from NH(X,0) needing 3.8–4.0 eV will be excited by the $N_2$(X,v = 14–15) energy levels.

Then the following reaction will be exothermic:

$$N_2(X, v > 13) + NH \rightarrow N_2 + NH(A, v = 0) \quad (12)$$

The rate coefficient of reaction (12) is unknown. $k_f = 4 \times 10^{-11}$ cm$^3$ s$^{-1}$ is chosen as for the two exothermic reactions: $N_2$(X, v > 13) + $N_2$(A) → $N_2$ + $N_2$(B,11) and $N_2$(X, v > 13) + $N_2^+$ → $N_2$ + $N_2^+$(B) [6, 7] 12].

The $I_{336}$ intensity is then written as follows:

$$I_{336} = c(336) \cdot (hc/336)A(336) \cdot [X, v > 13] \cdot [NH].k_f / \left( v^R_{NH,A} + [M] \cdot k^M_{NH,A} \right) \quad (13)$$

where $c(336)$ is the spectral response of the used monochromator, $A(336) = \nu^R{}_{NH,A} = 2 \times 10^6$ s$^{-1}$ [16], $k_f = 4 \times 10^{-11}$ cm$^3$ s$^{-1}$ and $k^M{}_{NH,A}$ is the quenching rate of the NH(A) state by the M molecules. In [16], it is reported that $k^{N2}{}_{NH,A} < 5 \times 10^{-14}$ cm$^3$s$^1$ and $k^{H2}{}_{NH,A} = 5 \times 10^{-11}$ cm$^3$ s$^{-1}$.

The line ratio method is applied to determine the NH radical relative density from the following $a_{N+N}.I_{580}/I_{336}$ intensity ratio, calculated with eqs. (4) and (13) at 2 Torr [13]:

$$a_{N+N} \cdot I_{580}/I_{336} = 7.5 \times 10^{-7} [N^2]/[X, v > 13] \cdot [NH] \quad (14)$$

The H-atoms are related to NH by the reaction (11) and the following relationships see [17]:

$$N + NH \rightarrow H + N_2, \text{ with } k_g = 5 \times 10^{-11} cm^3 s^{-1} \quad (15)$$

$$N(^2D) + H_2 \rightarrow H + NH \quad (16)$$

$$H + NH \rightarrow H_2 + N \quad (17)$$

It comes:

$$[NH] = (k_e \cdot [H] \cdot [N] \cdot [N_2] + k_h \cdot [H_2] \cdot [N(^2D)]) / (k_g \cdot [N] + k_i \cdot [H]) \quad (18)$$

with $[H_2] = [H_2^0] - 1/2[H]$.

The NH(0–0)-(1–1) bands at 336–337 nm are intense as shown in Fig. 3. The NH(1–1) band at 337 is mixed with the $N_2$(0–0) band at 337 nm. Consequently, the $I_{336}$ intensity is chosen alone to detect the NH radical. It is measured from the middle of the $I_{336}$ and $I_{337}$ junction.

## Gas Temperature

The gas temperature $T_g$ in the discharges and afterglows was estimated by the $P_1/P_2$ intensity ratio of the first two rotational bands of the 1st positive emission at 775 nm [18]. If a hot temperature was found in the $N_2$ discharge ($T_g = 500$–$600$ K at 8 Torr, 1 slpm [19]), the room gas temperature (300 K) was measured in the present afterglows. Consequently, the rate coefficients above are taken at 300 K as for reaction (3) which is depending on gas temperature [10].

## The Experimental Results

In Table 1, the first and second lines show the results of active species density in mixed gas of $N_2$ and $H_2$(0–2.5%) with the Figs. 1 and 2 setups for the same plasma and afterglow conditions ($10^{-3}$ s, 0.5 Slpm, 200 Watt).

The N($^2$D) and H atom densities reported in Table 1 are deduced from Eq. 18 calculations as being the upper density limits to obtain a positive value of H and N($^2$D) densities.

In the two $N_2$-$<2.5\%H_2$ early afterglows of Figs. 1 and 2, identical values of N-atom densities which increased up to $0.4\%H_2$ from 5 to a maximum value of $7 \times 10^{14}$ $cm^{-3}$ were found. While between 0.4 and 1.0% of $H_2$, the density of the N-atoms slowly decreased. These results are similar to that of Ref. [3]. The weak maximum of the N-atom density at $x(H_2) = 0.4\%$ has been previously correlated to a best surface wettability.

For the other active species, lower densities were found with the Fig. 2 setup except for NH and H in $N_2$-$1\%H_2$.

By comparing the results obtained with the setup of Fig. 1 at $z = 3$ cm and of Fig. 2 in the 5 L reactor at the same afterglow times of $10^{-3}$ s (lines 1 and 2), it was observed with the setup of Fig. 2 an increase of the late afterglow condition by the $a_{N+N}$ factor. Keeping the same densities of N-atoms, a decrease of $N_2$(X, v > 13) density with $H_2$ and a reduction

**Table 1** A $a_{N+N}$ factors (from the $I_{11/9}$ band ratio) and active species densities along the 5 L diameter in the afterglows of $N_2$-$x$%$H_2$ with $x$ = 0–2.5%, $p$ = 2 Torr, $Q_{tot}$ = 0.5 slpm and 200 Watt

| $x$ (%) | | 0 | 0.1 | 0.4 | 1 | 2.5 |
|---|---|---|---|---|---|---|
| $a_{N+N}$ | Setup of Fig. 1—$10^{-3}$ s | 0.14 | 0.3 | 0.3 | *0.3* | 0.3 |
| | Setup of Fig. 2—$10^{-3}$ s | 0.5 | 0.70 | 0.85 | 0.9 | |
| [N] ($10^{15}$ cm$^{-3}$) | Setup of Fig. 1—$10^{-3}$ s | 0.5 | 0.5 | 0.7 | 0.6 | 0.5 |
| | Setup of Fig. 2—$10^{-3}$ s | 0.5 | 0.55 | 0.7 | 0.6 | |
| [$N_2$(X, v > 13)]($10^{13}$ cm$^{-3}$) | Setup of Fig. 1—$10^{-3}$ s | 5.5 | 3 | 5 | 6 | 5 |
| | Setup of Fig. 2—$10^{-3}$ s | 6 | 2.4 | 2 | 0.9 | |
| [$N_2^+$] ($10^{10}$ cm$^{-3}$) | Setup of Fig. 1—$10^{-3}$ s | 3 | 0.3 | 0.3 | 1 | 0.1 |
| | Setup of Fig. 2—$10^{-3}$ s | 0.3 | 0.05 | 0.04 | 0.1 | |
| [NH] ($10^9$ cm$^{-3}$) | Setup of Fig. 1—$10^{-3}$ s | | 0.15 | 0.13 | 0.14 | 0.15 |
| | Setup of Fig. 2—$10^{-3}$ s | | 0.04 | 0.07 | 0.12 | |
| [N($^2$D)]($10^{11}$ cm$^{-3}$) | Setup of Fig. 1—$10^{-3}$ s | | < 0.25 | < 0.08 | < 0.03 | < 0.01 |
| | Setup of Fig. 2—$10^{-3}$ s | | < 0.02 | < 0.02 | ≤ 0.02 | |
| [H] ($10^{13}$ cm$^{-3}$) | Setup of Fig. 1—$10^{-3}$ s | | < 0.2 | < 0.2 | < 0.2 | < 0.1 |
| | Setup of Fig. 2—$10^{-3}$ s | | ≤ 0.06 | ≤ 0.1 | ≤ 0.2 | |
| [H]/2[$H_2$]$^0$ | Setup of Fig. 1—$10^{-3}$ s | | < 20 $10^{-3}$ | < 4 $10^{-3}$ | < 2 $10^{-3}$ | < 0.6 $10^{-3}$ |
| | Setup of Fig. 2—$10^{-3}$ s | | < 1 $10^{-3}$ | < 1 $10^{-3}$ | < 2 $10^{-3}$ | |

of 10 times of $N_2^+$ ions density was noticed. The H-atom density was the same with 1%$H_2$ into $N_2$. Thus the Fig. 1 setup at $z$ = 3 cm was in favour of $N_2^+$ ions.

Table 2 shows the comparison of the results in pure $N_2$ at 2 Torr, obtained with the setups of Fig. 1 at $10^{-3}$ s ($z$ = 3 cm—line 1) and at $10^{-2}$ s (across the 5 L reactor—line 2).

In the Fig. 1 setup a constant N-atom density is kept from an afterglow time of $10^{-3}$ s and $10^{-2}$ s in that a huge reduction, at time $10^{-2}$ s by a factor 10 for $N_2$(X,v > 13) and $10^2$ for $N_2^+$ active species density, were observed. A long afterglow time in the Fig. 1 setup ($10^{-2}$ s) is thus detrimental to high $N_2$(X, v > 13) and $N_2^+$ active species density in the 5 L reactor. Such a result comes from the very low destruction probability of N-atoms on the tube wall ($\gamma = 10^{-4}$–$10^{-5}$) in comparison to those of $N_2$(X, v > 13): $\gamma = 10^{-2}$–$10^{-3}$ for $N_2$(X,v > 13) [4] and a full wall recombination for $N_2^+$.

For a surface treatment with high densities of $N_2$(X, v > 13) and $N_2^+$ added to constant N and H atoms, the Fig. 2 setup, with an afterglow time of $10^{-3}$ s, appears to be the most appropriate setup. Still higher $N_2^+$ ions density should be obtained inside the 18 mm diameter tube, before the 5 L reactor, where a sample could be introduced.

To increase the $H_2$ dissociation rate, the afterglows of Ar-$N_2$-$H_2$ gas mixtures of Ar-$N_2$-$H_2$ gas mixtures specifically the Ar-2%($N_2$-5%$H_2$) has been studied [13, 20, 21]. The

**Table 2** A $a_{N+N}$ factors and active species densities in the $N_2$ afterglows of Fig. 1 at times $10^{-3}$ s and $10^{-2}$ s at $p$ = 2 Torr, $Q_{tot}$ = 0.5 slpm and 100 Watt

| | $a_{N+N}$ | [N] ($10^{15}$ cm$^{-3}$) | [$N_2$(X,v > 13)] ($10^{13}$ cm$^{-3}$) | [$N_2^+$] ($10^{10}$ cm$^{-3}$) |
|---|---|---|---|---|
| Setup of Fig. 1—$10^{-3}$ s | 0.14 | 0.5 | 5.5 | 3 |
| Setup of Fig. 1—$10^{-2}$ s | 0.85 | 0.5 | 0.5 | 0.04 |

plasma length increased from 4 cm with $N_2$–x$H_2$ to 20 cm with a 98%Ar dilution. Then a jet was observed at 2 Torr inside the 5 L reactor. The present optical measurement was performed 2 cm above the jet, expecting a full afterglow diffusion inside the 5 L reactor.

In $N_2$ at 4 Torr, 1 slpm, 100 Watt, an afterglow time of 3 $10^{-3}$ s, a $N/N_2$ ratio higher than 10% has been previously observed [5].

In the Ar-2%$N_2$-$10^{-3}$ $H_2$ gas mixture at 2 Torr, 1 Slpm, 150 Watt, afterglow time of 1 $10^{-3}$ s, it has been measured with the Fig. 2 setup in the 5 L reactor: $[N] = 2 \times 10^{14}$ $cm^{-3}$, $[N_2, v > 13] = 0.4 \times 10^{13}$ $cm^{-3}$, $[N_2(A)] = 1.7\ 10^{10}$ $cm^{-3}$, $[N_2^+] = 2 \times 10^9$ $cm^{-3}$, $[NH] = 0.2 \times 10^9$ $cm^{-3}$, $[H] \leq 0.4 \times 10^{13}$ $cm^{-3}$. The corresponding $[N]/[N_2]$ and $[H]/[H^0{}_2]$ ratios were 15% and ≤ 6% respectively. By comparison in $N_2$-(0.4–1)%$H_2$, 2 Torr, 0.5 slpm, 200 Watt (Table 1), there is thus a sensitive increase of the $[N]/[N_2]$ and $[H]/[H^0{}_2]$ ratios with the 98%Ar dilution.

## Conclusion

By connecting the diameter 5 mm discharge tube directly to the 5 L reactor, an homogenous short afterglow (SA of $10^{-3}$ s) in the whole 5 L reactor with the mixed gas of $N_2$ and $H_2$(0–2.5%) at 2 Torr, 0.5 slpm, 200 Watt was obtained. By comparison with a 1.8 cm diameter early afterglow in the same plasma and afterglow time condition of $10^{-3}$ s, the part of the N + N recombination in the 5 L afterglow increased, with a N-atom density unchanged and a dissociation rate $N/2N_2 = (5–7) \times 10^{-3}$. By considering a rate coefficient $k_c = 4 \times 10^{-11}$ $cm^3$ $s^{-1}$ for the $N_2(X, v > 13) + NH$ reaction, the $H/2H^0{}_2$ dissociation rates were found to be ≤ (1–4) × $10^{-3}$ in the same range for the two considered setup.

The purpose of using a direct connection of 5 mm diameter discharge tube to the 5 L reactor was to obtain a more efficient surface treatment in a short afterglow (SA of $10^{-3}$ s) with more $N_2(X, v > 13)$ and $N_2^+$ active species than in a long afterglow (LA of $10^{-2}$ s). For the experimental conditions of $N_2$-1%$H_2$ at 2 Torr, 0.5 slpm, the $N/N_2$ and H/N ratios had constant values of 1% and 0.3% respectively.

To increase the N and H atom densities, an Ar-2% $N_2$-$10^{-3}H_2$ gas mixture was experimented, giving in the 5 L reactor $N/N_2$ and H/N ratios of 7.5% and 2%, nearly one order of magnitude higher than in $N_2$-(0.4–1)%$H_2$.



## References

1. Villeger S, Cousty S, Ricard A, Sixou M (2003) Sterilization of *E. coli* bacterium in a flowing $N_2$–$O_2$ post-discharge reactor. J Phys D Appl Phys 36:L6
2. Villeger S, Sarrette JP, Rouffet B, Cousty S, Ricard A (2008) Treatment of flat and hollow substrates by a pure nitrogen flowing post discharge. Application to bacterial decontamination in low diameter tubes. Eur Phys J Appl Phys 42:25–32

3. Abdeladim M, Sarrette JP, Ricard A, Mekkakia Maaza N (2014) Production of active species in $N_2$–$H_2$ microwave flowing discharges and afterglows: application to change of paper surface wettability. Eur Phys J Appl Phys 67:10801
4. Ricard A, Sarrette JP, Oh SG, Kim YK (2016) Comparison of the active species in the RF and microwave flowing discharges of $N_2$ and Ar-20%$N_2$. Plasma Chem Plasma Process 36:1559–1570
5. Ricard A, Zerrouki H, Sarrette JP (2015) Determination of N and O-atoms, of $N_2$(A) and $N_2$(X, v>13) metastable molecules and $_N{}^2$+ ion densities in the afterglows of Ar-$_N$2 microwave discharges. J Anal Sci Methods I 5:59–65
6. Zerrouki H, Ricard A, Sarrette JP (2013) Determination of N and O-atoms and $N_2$(A) metastable molecules densities in the afterglows of $N_2$ and $N_2$–$O_2$ (1) and $N_2$–$H_2$, Ar-$N_2$-$H_2$ and Ar-$N_2$-$O_2$ (2) microwave discharges. Contrib Plasma Phys 53:599–604
7. Zerrouki H, Ricard A, Sarrette JP (2014) Determination of N and O-atoms and $N_2$(A) metastable molecules densities in the afterglows of $N_2$ and $N_2$–$O_2$ (1) and $N_2$–$H_2$, Ar-$N_2$-$H_2$ and Ar-$N_2$-$O_2$ (2) microwave discharges. Contrib Plasma Phys 54:827–837
8. Laux CO, Kruger CH (1992) Arrays of radiative transition probablities for the $N_2$ first and second positive, NO beta and gamma, $N_2{}^+$ first negative and $O_2$ schumann-runge band systems. J Quant Spectrosc Radiat Transf 48:9
9. Gilmore FR, Laher RR, Espy PJ (1992) FC-factors, r-Centroïds, Electronic transitions moments and Einstein coefficients for many $N_2$ and $O_2$ band systems. J Phys Chem Ref Data 21:1005
10. Kossyi IA, Kostinsky AY, Matveyev AA, Silakov VP (1992) kinetic schemen of the non-equilibrium discharge in nitrogen-oxygen mixtures. Plasma Sourc Sci Technol 1:207
11. Shemansky DE (1976) $A^3\sum_u{}^+$ molecules in the $N_2$ afterglow. J Chem Phys 64:565
12. Ricard A, Oh SG, Guerra V (2013) Line-ratio determination of atomic oxygen and $N_2$(A) metastable absolute densities in an RF nitrogen late afterglow. Plasma Sour Sci Technol 22:035009
13. Ricard A, Amorim J, Abdeladim M, Sarrette JP (2020) High H-atom density in R(He, Ar)/x%(N2–5%H2) early afterglows. Plasma Chem Plasma Process 40:1559–1570
14. Brown RL (1973) "A measurement of the rate of the reaction N + H + M → NH + M. Int J Chem Kin 5:663
15. Hayden Smith W, Brzozowski J, Erman P (1976) Lifetime studies of the NH molecule: new predissociations, the dissociation energy, and interstellar diatomic recombination. J Chem Phys 64:4628
16. Hofzumahaus A, Stuhl F (1985) Electronic quenching, rotational relaxation, and radiative lifetime of NH($A\ ^3\Pi$, $v$'=0, $N$'). J Chem Phys 82:3152
17. Tatarova E, Dias FM, Gordiets B, Ferreira CM (2005) Molecular dissociation in $N_2$–$H_2$ microwave discharges. Plasma Sour Sci Technol 14:19
18. Britun N, Gaillard M, Ricard A, Kim YM, Kim KS, Han JG (2007) Determination of the vibrational, rotational and electron temperatures in $N_2$ and Ar-$N_2$. J Phys D Appl Phys 40:1022
19. Ricard A, Sarrette JP, Oh SG, Kim YK (2016) Comparison of the active species in the RF and microwave flowing discharges of $N_2$ and Ar-$N_2$. Plasma Chem Plasma Process 36:1559
20. Ricard A, Sarrette JP (2019) Active species densities in R/x%N2 and R/x%(N2–5%H2)(R=Ar, He) microwave flowing afterglows. J Phys Conf Ser 1243:012001
21. Ricard A, Sarrette JP (2019) Densities of active species in R/x%(N2–5%H2) (R = Ar or He) microwave flowing afterglows. Plasma Chem Plasma Process 39:1103